Journal of Metals, Materials and Minerals, Vol. 30, No. 4, pp. 30-38, 2020

Characterization of TiO_2-activated carbon onto adsorption and photocatalytic properties and its application

Mark CHOBCHUN[1], Pasakorn JUTAKRIDSADA[1], Puttiporn THIAMSINSANGWON[2], Pornnapa KASEMSIRI[1], Khanita KAMWILAISAK[1,3*], and Prinya CHINDAPRASIRT[3]

[1] *Department of Chemical Engineering, Faculty of Engineering, Khon Kaen University, Khon Kaen, 40002, Thailand*
[2] *Department of Chemical and Material Engineering, Faculty of Engineering, Rajamangala University of Technology Thanyaburi, Pathum Thani 12110, Thailand*
[3] *SIRDC-Sustainable Infrastructure Research and Development, Department of Civil Engineering, Faculty of Engineering, Khon Kaen University, Khon Kaen, 40002, Thailand*

***Corresponding author e-mail**: khanita@kku.ac.th

Received date:
7 May 2020
Revised date
21 September 2020
Accepted date:
22 September 2020

Keywords:
Titanium dioxide;
Activated carbon;
Nanocomposite;
Photocatalyst;
Synergic effect

Abstract

This study investigates the characterization of TiO_2 in conjunction with activated carbon (AC) on its adsorption and photocatalytic properties. TiO_2 in the absence and presence of AC were prepared by the sol-gel method. $TiCl_4$ was used as a precursor to reduce using acidic solution during preparation process. The effects of the amount of AC on the characteristics of composites were investigated. TGA technique was used to evaluate the amount of TiO_2 and AC in TiO_2/AC composite. The adsorption properties of TiO_2/AC were characterized using XRD, TEM, N_2 adsorption/desorption, FTIR and UV–Vis diffuse reflectance spectroscopy techniques. The photocatalytic activities of the composites were investigated by measuring the removal of acid dye. Results showed that the specific surface area of TiO_2/AC increased with increasing mass fraction of AC, while the energy band gap was reduced. It was clearly shown that TiO_2 in the presence of AC produced a synergistic effect of the composite and led to an increase in photocatalytic performance. Also, the reuse of TiO_2 with 20% AC nanocomposites for dye removal showed a high reuse efficiency above 90% in photocatalytic dye degradation.

1. Introduction

Recently, TiO_2 photocatalysis has been widely used in the environmental purification due to its being an inexpensive, strongly oxidizing and highly stable chemical [1]. It is also capable of the photo-oxidative destruction of most organics pollutants [1-5] to CO_2 and H_2O. However, the drawback of this catalyst is the difficulty in the separation and retrieval after the use in photocatalytic systems [6]. Although such problem has been solved by immobilizing the photo-catalyst on porous supports, such as porous alumina ceramic [7], carbon foam and cordierite foam [8], the advantage of recombination of materials is not adequately displayed on the photocatalytic degradation of pollutants [9].

It has been reported that TiO_2 when loaded with activated carbon (AC), can enhance the photocatalytic activity of TiO_2. This is because AC increases the adsorption of organic pollutant on TiO_2/AC, leading to a high organic concentration around TiO_2. While AC has no photocatalytic activity, the system exhibits synergism in which the adsorbed organic molecules on AC are transferred to TiO_2 where they are degraded [4,10-12]. Furthermore, the synergistic effect of adsorption by AC and TiO_2 particulates can have beneficial consequences in the photodegradation of a dye in aqueous media [13].

Due to the desirable properties described above, the TiO_2 with AC composites prepared by the sol-gel method to enhance the catalytic properties was proposed. The effects of AC content on the physical and chemical properties of TiO_2/AC composites were investigated. The key objective was to evaluate the efficiency of dye degradation using TiO_2/AC in various experiment configurations. Besides, the reuse of TiO_2/AC nanocomposite for dye removal was determined.

2. Materials and method

2.1 Materials

Titanium tetrachloride ($TiCl_4$) from Merck Company (Germany); titanium dioxide (TiO_2) (COM-grade) Degussa P25 from Sigma-Aldrich Co. Ltd (Thailand); ammonium hydroxide (NH_4OH) from Ajax Finechem Company (Australia); activated charcoal (AR-grade) from Rankem (India) and yellow acid dyes (COM-grade) from Phua Kiam Seen Co. Ltd. were used in this work. For water, deionized water was used in all experiment.

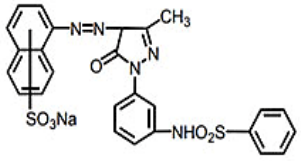

Scheme 1. Yellow acid dye structure

 DOI: 10.14456/jmmm.2020.xx

2.2 TiO_2/AC composite catalyst preparation

TiO_2/AC composite was prepared by the sol-gel technique. Ten millilitres of titanium tetrachloride ($TiCl_4$) was slowly dropped into forty millilitres of deionized water at 4±1°C with continuous stirring. Titanium hydroxide ($Ti(OH)_4$) solution or sol was obtained. Various amounts of activated charcoal (0, 5, 10, 20, 25 and 30 wt% of AC) were put into the sol. A droplet of 30% v/v of ammonium hydroxide (NH_4OH) was continuously added until the gel was formed. The gel was then washed with distilled water and dried in the oven at 100°C for 4 h. The dried gel of TiO_2 and TiO_2/AC were heated in a nitrogen atmosphere to 500°C at heating rate of 10°C·min^{-1}. The sample was dried for further 4 h at 500°C. At 500°C, the anatase phase of TiO_2 can be formed. However, the slight decompose of AC was observed at 500°C about 5%. This value was in acceptable for using AC support for catalyst. The TiO_2/AC samples with various amounts of AC (0, 5, 10, 20, 25 and 30 wt%) were named TiO_2, TiO_2/5AC, TiO_2/10AC, TiO_2/20AC, TiO_2/25AC, and TiO_2/30AC.

2.3 Characterization

The thermal decomposition of the composite was determined by thermalgravimetric analysis (TGA) (TGA 50, Shimadzu, Japan). A 200 mg sample of prepared composites was heated in a range of 30-750°C with a heating rate of 10°C·min^{-1} under a nitrogen flow. Crystalline structure and morphology of TiO_2/AC composite were examined by X-ray diffraction powder (a Bruker D8-Advance), and Transmission Electron Microscopy (TEM, model Tecnai™ G^2 20, FBI, USA).

The specific surface area and pore volume of the composite were determined by Nitrogen adsorption-desorption isotherms measured by gas sorption analyzer (micromeritics ASAP 2010) [15]. Before the adsorption measurement, the samples were degassed at 110°C under vacuum (<50 mmHg) for 12 h. The nitrogen adsorption/ desorption isotherms were recorded at the liquid nitrogen temperature. The specific surface area, S_{BET}, was calculated using the Brunauer-Emmet-Teller (BET) method. The micropore volume, V_{mic}, was calculated using the Dubinin-Radushkevich (DR) equation. The total pore volume, V_T, was found from the amount of N_2 adsorbed at the relative pressure of 0.99. The mesopore and macropore volume, $V_{meso+mac}$, was obtained by subtraction of the micropore volume from the total pore volume. The average pore diameter, D_p, was calculated from $(4\times V_T)/S_{BET}$.

The composites were examined by FTIR analysis on a VERTEX 70 spectrometer over the wave number of 3800-400 cm^{-1} using KBr pellets for sample preparation. The UV–Vis diffuse reflectance spectra were recorded with a UV-3600 SHIMADZU (Japan) spectrometer in the wavelength of 800-200 nm. The absorption edge and bandgap energies of the as-prepared samples were determined by UV–Vis diffuse reflectance spectroscopy (Analytik Jena GmbH, Germany).

2.4 Photocatalytic activity test

Catalytic activity tests were conducted in a batch reactor (1000 mL) with magnetic stirrer running at 200 rpm. The 500 mL reaction mixture contained 1.0 g·L^{-1} of TiO_2/AC with 70 mg·L^{-1} of dye concentration. The reaction mixture was kept in dark condition to reach an adsorption equilibrium for 15 min. The photocatalytic reaction was then carried out with 365 nm UV-light source (Haining Guanyi Electrical Co., Ltd). The sample was kept in the reactor for 0, 5, 10, 15, 30, 45, 60, 90, 120, 150 and 180 min. The concentration of dye solution was measured by UV–Vis Spectrophotometer at 396 nm. The percentage of dye removal was calculated by:

$$\%Dye\ removal = \frac{(C_0 - C_t)}{C_0} \times 100 \quad (1)$$

where C_0 and C_t are acid dye concentrations (mg·L^{-1}) at time *0* and time *t*, respectively.

Langmuir-Hinshelwood model has been used to evaluate the kinetic order of dye photodegradation. This model could be modified to be a pseudo-first order rate equation that apparent rate constants (k_{app}) of the samples are calculated as follows [16]:

$$In\frac{C_t}{C_0} = k_{app}t \quad (2)$$

where t is the irradiation time.

3. Result and discussions

3.1 TGA analysis

TGA technique was used to evaluate the amount of TiO_2 and AC in TiO_2/AC composite. The results of TGA, as shown in Figure 1 showed that the AC thermally decomposed under N_2 condition from 520 to 660°C. The weight loss of AC was approximately 99% at 660°C. On the other hand, TiO_2 was more thermal stable with a small weight loss of 2.06% from the start to 700°C. Thus, the weight fraction of TiO_2 to AC ratio was calculated. Figure 1 shows the weight fraction of TiO_2/AC composite. The ratios of TiO_2 to AC of TiO_2/5AC, TiO_2/10AC TiO_2/20AC TiO_2/25AC and TiO_2/30AC samples were 85:15, 83:17, 67:43, 18:82 and 15:85, respectively. The weight fraction of TiO_2 to AC was not the same as that of the initial preparation ratios due to the loss of $Ti(OH)_4$ during the preparation process.

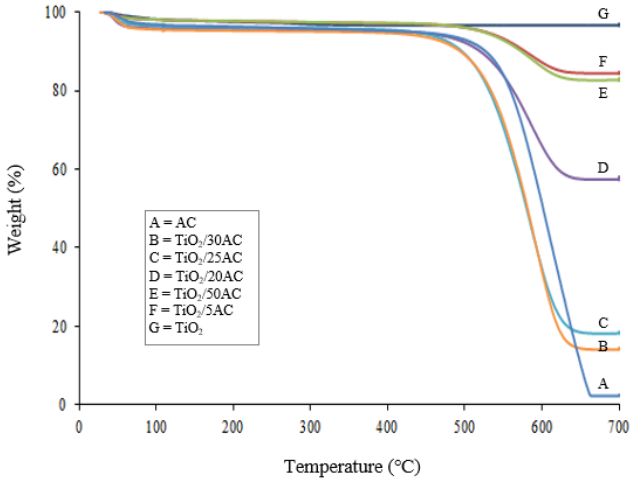

Figure 1. TGA of activated carbon (AC), Titanium dioxide (TiO_2), and TiO_2/AC composites.

3.2 XRD analysis

XRD patterns of AC, TiO_2 and TiO_2/AC are shown in Figure 2. TiO_2 and TiO_2/AC composites showed peaks of a nanocrystalline product of anatase (a form of TiO_2) as the only phase present. The highest peak was found at 25.29° as (101) plane. This was due to the heat treatment at 500°C, which is known to produce high anatase content [17]. Calcination at 500°C was used in this work because anatase has a better photocatalytic activity due to the higher electron-hole pair lifetime compared to rutile [18]. However, the sample TiO_2/25AC and TiO_2/20AC showed the presence of rutile peak at about 27°, it may be the presence of AC which could effect during phase transformation [19]. For AC sample, there was no peak in the XRD pattern. For TiO_2/AC composites, the peak intensity gradually decreased with an increasing amount of AC. The crystalline sizes of synthesized samples were in the range of 5-10 nm (supplementary data Table S.1) which was obtained from Scherrer's equation [20, 21].

$$D = \frac{K\lambda}{\beta \cos\theta} \quad (3)$$

where λ (wavelength of X-Ray) = 0.15418 nm, β = full width and half maxima, θ = Bragg's angle (2θ = 25.15°). D = Crystallite size, K = Scherrer constant (0.089), and B = the line width at half-maximum height, after substraction of equipment broadening.

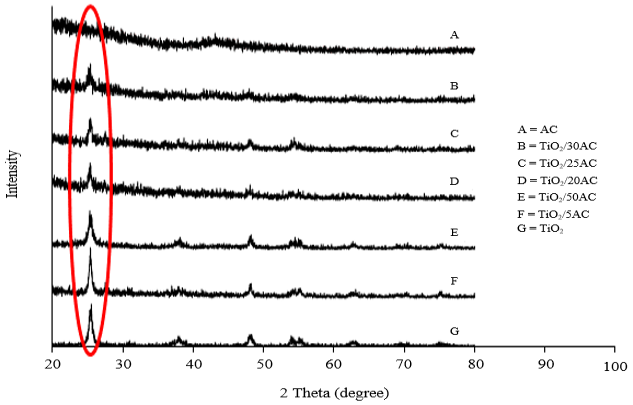

Figure 2. XRD pattern of activated carbon (AC), Titanium dioxide (TiO_2), and TiO_2/AC composites.

3.3 TEM analysis

Figure 3 shows a typical TEM image of TiO_2, AC and TiO_2AC samples. The TiO_2 nanocrystals (Figure 3(a)) were tetragonal in shape, and the particle sizes were 10-15 nm in diameter, which are the characteristics of anatase structure [22]. Furthermore, from Figure 3 (b-d), all TiO_2/AC composites showed similar morphology to that of TiO_2 due to the same preparation conditions. The particle sizes obtained from TEM. were similar to those obtained from XRD.

3.4 BET analysis

Figure 4 shows the results of N_2 adsorption-desorption isotherms. The AC isotherm was the typical type I isotherm based on IUPAC (International Union of Pure and Applied Chemistry) classification and corresponded to unimolecular adsorption [23]. The isotherms rose sharply at the beginning of adsorption due to the micropore filling effect. After that, the adsorption of N_2 became constant. This result indicated the microporosity of the AC sample. The TiO_2 and TiO_2/AC isotherms are the typical type IV isotherm mostly found in mesoporosity materials of 2-50 nm in diameter [24]

However, the ratio of TiO_2 to AC had a considerable influence on the type of adsorption isotherm. The increased amount of AC tended to change the type IV isotherm to the typical type I isotherm. Table 1 gives a summary of the results of BET surface area ($m^2 \cdot g^{-1}$), total pore volume ($cm^3 \cdot g^{-1}$) and average pore diameter (Å) AC. The specific surface area, total pore volume and average pore diameter of TiO_2 were 56.09 $m^2 \cdot g^{-1}$, 0.12 $cm^2 \cdot g^{-1}$ and 85.26 Å, respectively and those of AC were 925.12 $m^2 \cdot g^{-1}$, 0.61 $cm^2 \cdot g^{-1}$ and 26.24 Å, respectively. The BET surface area and total pore volume increased significantly with an increasing amount of AC while the average pore diameter decreased sharply. However, it can be noticed that the average pore diameter of TiO_2/30AC was similar to AC, while the specific surface area of TiO_2/AC composite was related to the ratio of TiO_2 to AC.

The calculated specific surface area can be obtained from mass fraction and measured specific surface area of TiO_2 and AC from the following equation.

$$Calculated\ specific\ surface\ area = S_{BET,TiO_2} V_{TiO_2} + S_{BET,AC} V_{AC} \quad (4)$$

where S_{BET,TiO_2} and $S_{BET,AC}$ are specific surface areas of TiO_2 and AC measured from Nitrogen adsorption-desorption, and V_{TiO_2} and V_{AC} are mass fractions of TiO_2 and AC obtained from TGA analysis.

The calculated specific surface area of TiO_2/AC is also shown in Table 1. It can also be observed that the calculated specific surface area of TiO_2/AC was similar to the BET specific surface area due to the excellent distribution of TiO_2 in AC.

Table 1. Surface area, pore and energy band gap of TiO_2 (P25) TiO_2, AC and TiO_2/AC composite.

Materials	BET surface area ($m^2 \cdot g^{-1}$)	Calculated surface area ($m^2 \cdot g^{-1}$)	Total pore volume ($cm^3 \cdot g^{-1}$)	Average pore diameter (Å)	Energy Band gap, Eg (eV)
TiO_2 (P25)	-	-	-	-	2.96
TiO_2	56.09	56.09	0.12	85.26	2.99
TiO_2/5AC	151.02	147.18	0.24	64.36	2.27
TiO_2/10AC	265.40	203.83	0.29	43.81	2.15
TiO_2/20AC	475.69	421.08	0.33	27.89	1.80
TiO_2/25AC	703.06	760.00	0.56	30.71	1.41
TiO_2/30AC	784.13	803.46	0.53	26.94	1.13
AC	925.12	925.12	0.61	26.23	1.03

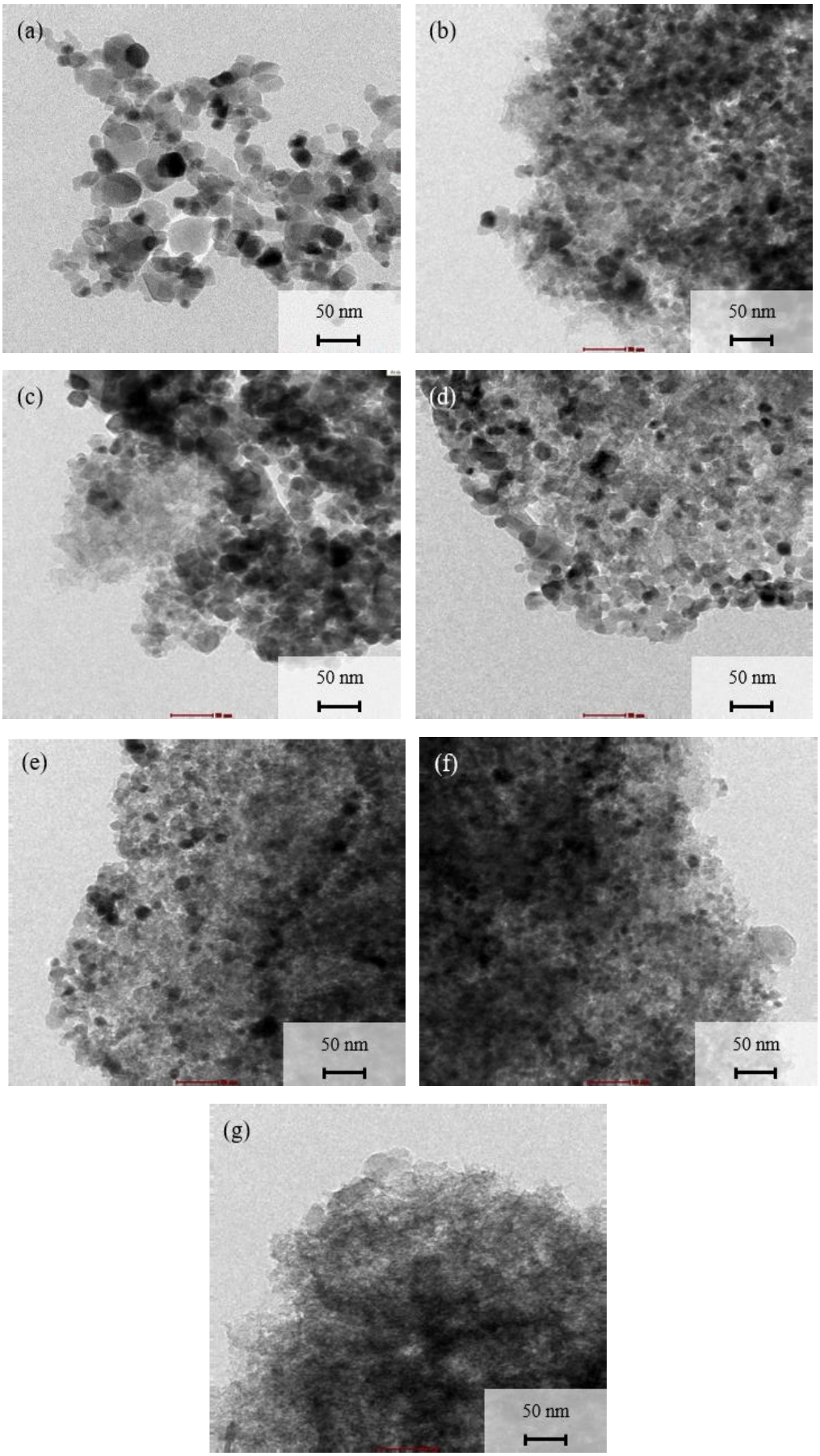

Figure 3. TEM image of (a) TiO_2, (b) TiO_2/5AC, (c) TiO_2/10AC (d), TiO_2/20AC (e), TiO_2/25AC (f), TiO_2/30AC, and , (g) AC.

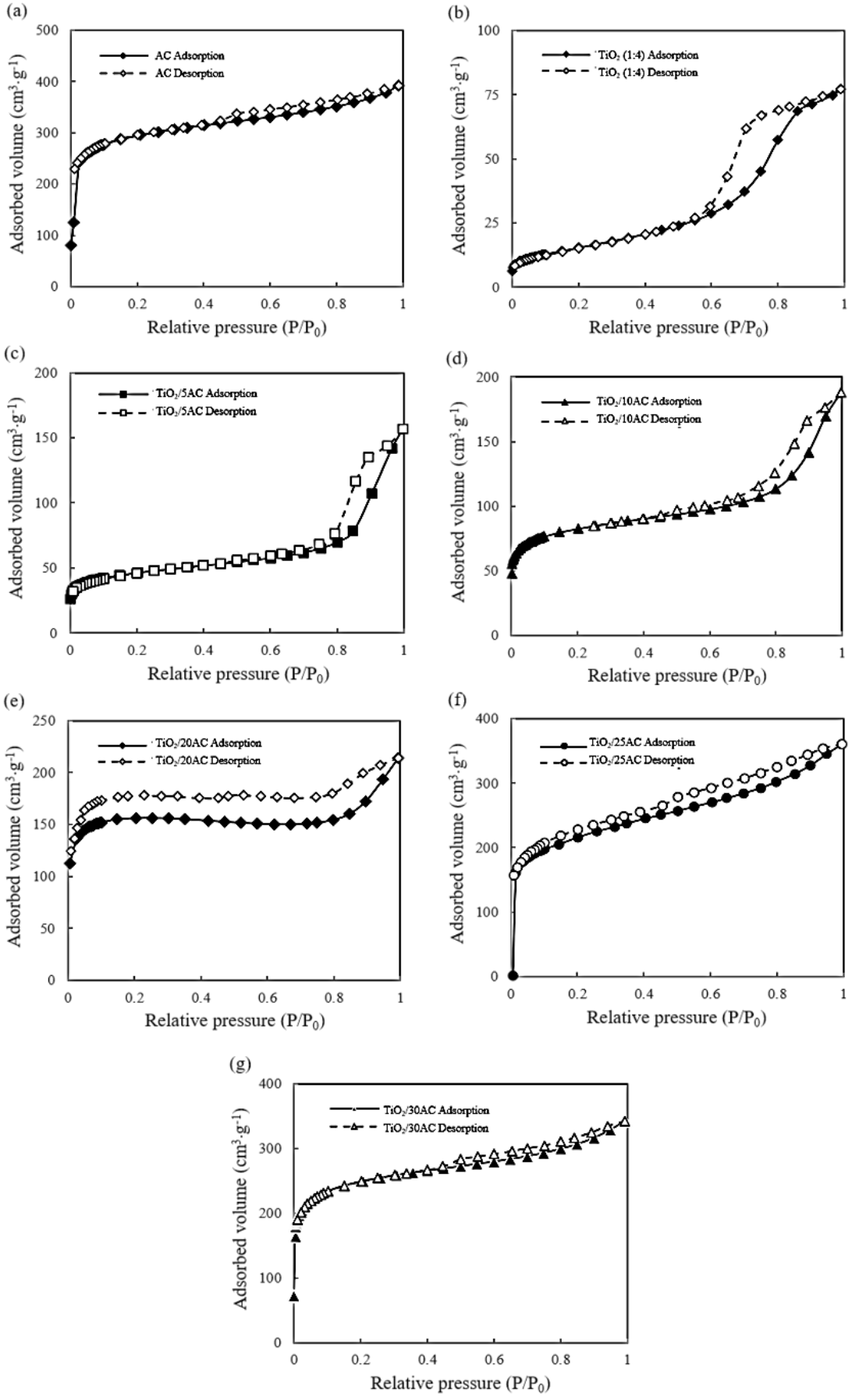

Figure 4. Adsorption/desorption isotherms of N_2 at 77 K of (a) AC, (b) TiO_2, (c) TiO_2/5AC, (d) TiO_2/10AC, (e) TiO_2/20AC, (f) TiO_2/25AC, and (g) TiO_2/30AC.

3.5 FTIR analysis

Figure 5 shows FTIR spectra of TiO_2, AC and TiO_2/AC. The prominent absorption peaks were at 2632, 2378, 2111, 1994, 1885, 1031 and 667 cm^{-1}. The band at 2292 cm^{-1} was assigned to -C≡C- alkynes stretching with and the band at 1250 cm^{-1} to aliphatic C-N amines stretching. Furthermore, all TiO_2/AC showed peaks at 1046 cm^{-1} corresponding to the Ti-O-C vibration band. The peak intensity increased with the increase in carbon contents. The result was similar to Liu *et al.* [10] and Perrin *et al.* [25] who reported that the electron affinity of C and Ti–O illustrated peak intensity in the range of 1038-1060 cm^{-1}. This was the evidence of carbon incorporating into the framework of titanium dioxide.

3.6 UV–vis-DRS analysis

Figure 6 shows the UV–Vis diffuse reflectance spectra of the TiO_2, AC, and TiO_2/AC composite. The TiO_2 (Degussa, P25), TiO_2, TiO_2/5AC, TiO_2/10AC and TiO_2/20AC spectra showed a characteristic absorbance around 320-420 nm indicating the existence of highly crystallized TiO_2. For the higher AC contents TiO_2/25AC, TiO_2/30AC

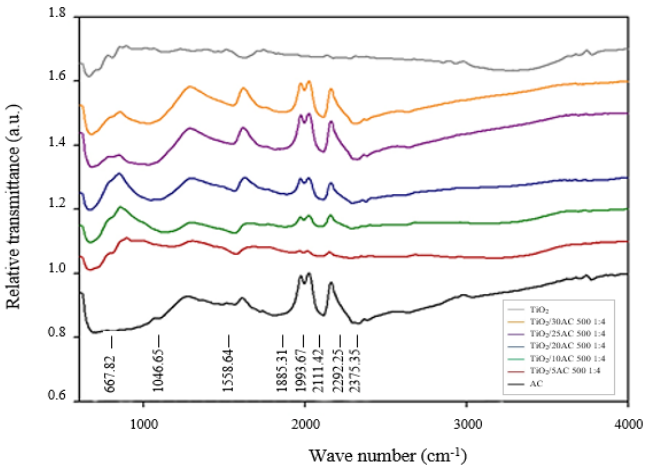

Figure 5. FTIR spectra of TiO_2, TiO_2/5AC, TiO_2/10AC, TiO_2/20AC, TiO_2/25AC, TiO_2/30AC and AC.

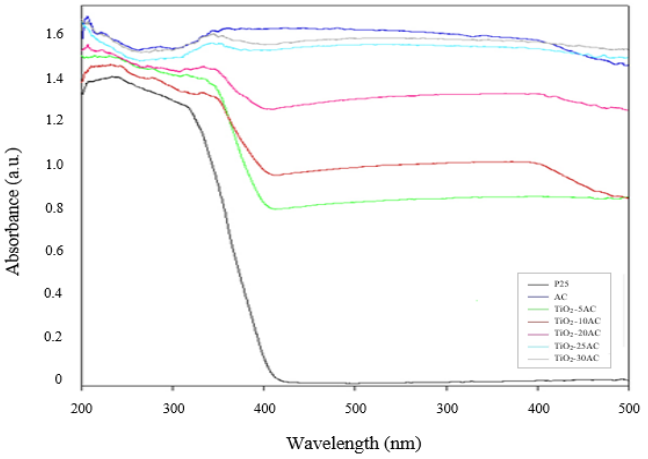

Figure 6. UV-Vis spectra of TiO_2, TiO_2/5AC, TiO_2/10AC, TiO_2/20AC, TiO_2/25AC, TiO_2/30AC and AC.

composites and AC, the spectra absorbance were relatively flat around 320-700 nm. This could be the effect of carbon molecules which would absorb in both UV and visible lights. An energy band gaps of the TiO_2 AC and TiO_2/AC nanocomposite were determined by graph plots of the Kubelka–Munk remission function for each nanocomposite (Figure S.1-S7.). The energy band gap is presented in Table 1. It can be seen that EG of TiO_2 prepared with the sol-gel technique was about 2.96 eV while Eg of TiO_2 (P25) was 2.99 eV. The bandgap of TiO_2/5AC, TiO_2/10AC, TiO_2/20AC, TiO_2/25AC TiO_2/30AC nanocomposites and AC were determined as 2.27, 2.15, 1.80, 1.41 1.13 and 1.03 eV, respectively. The reducing of bandgap could be attributed to the slight conjugation effect between Ti-O and carbon nanoparticle molecules (C). It can be noticed here that AC could enhance solar photocatalytic activity [26].

3.7 Dye removal

Figure 7 presents the percentage of dye removal by AC, TiO_2/5AC and TiO_2/10AC under UV-irradiation and dark condition. The percentage of dye removal was significantly increased with increasing time. The dye removal by AC reached 75% at 10 min and then remained constant, while those of TiO_2/5AC and TiO_2/10AC under dark condition were 52 and 72% at 180 min, respectively. The dye reduction by TiO_2/5AC and TiO_2/10AC in the presence of UV light was improved by 10 and 20% due to the photocatalytic reaction. TiO_2 in the presence of AC removed dye by adsorption up to approximately 30 min, and then the photocatalytic reaction phenomena occurred. Comparing the activity of AC, TiO_2, commercial TiO_2 (P25) and TiO_2/ 10AC, the fastest dye treatment was AC with 75% removal. It was known the physical treatment was fast and straightforward; however, the adsorption capacity depended on the quantity of adsorbent.

In case of TiO_2, the photocatalytic removal activity of TiO_2 (P25) was 57%, and that of as-prepared TiO_2 was 26% at reaction time 180 min. The better removal activity of TiO_2 P25 was primarily due to its smaller particle size than that of as-prepared TiO_2. The maximum dye removal of 88% was obtained with TiO_2/10AC under UV light. It was seen that TiO_2 in the presence of AC and UV light could significantly improve the dye removal. This confirmed the synergistic effect of TiO_2 and AC [27,28]. Furthermore, based on the literature, the physical mixture of the prepared TiO_2 and AC has been reported lower dye removal efficiency than that of the deposited TiO_2 on AC. This is because, in the physical mixture system, AC adsorbs dye and then desorbed, the photocatalytic reaction by TiO_2 begun to degrade dye from the bulik solution after absorption equilibrium, while in the deposited TiO_2/AC, the dye can be absorbed by AC and then directly reacted by TiO_2.This could be the benefit of the deposited TiO_2/AC in much faster photocatalytic rate and better performance [29].

3.8 Kinetic analysis of dye degradation

Based on equation (2), the straight-line relationship of $In\frac{C_t}{C_0}$ against reaction time was obtained, as shown in Figure S10 (supplement data). The apparent rate constants (k_{app}) and half-life time of each catalyst with an initial dye concentration of 75 mg·L^{-1} was calculated from the slope of the plot. The kinetic values are presented in Table 2.

Table 2. Kinetic values of TiO_2 (P25) TiO_2, AC and TiO_2/AC composite for dye removal.

Sample	k_{app} (min^{-1})	$t_{1/2}$ (min)	Regression coefficient (R^2)
AC	0.0311	22.29	0.9789
TiO_2 (P25)	0.0045	154.03	0.9838
TiO_2	0.0015	462.10	0.9848
TiO_2/5AC	0.0041	169.06	0.9595
TiO_2/10AC	0.0096	72.20	0.9727
TiO_2/20AC	0.0889	7.80	0.9515
TiO_2/25AC	0.224	3.09	0.9525
TiO_2/30AC	0.2352	2.95	0.7987

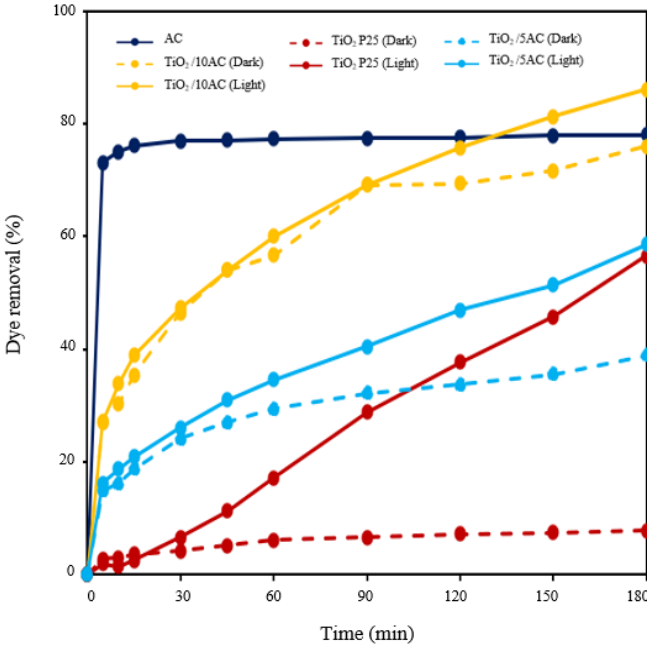

Figure 7. Dye removal of AC, TiO_2 P25, TiO_2/5AC and TiO_2/10AC with optimal conditions (acid dye concentration 75 $mg{\cdot}L^{-1}$ and catalytic loading 1.0 $g{\cdot}L^{-1}$).

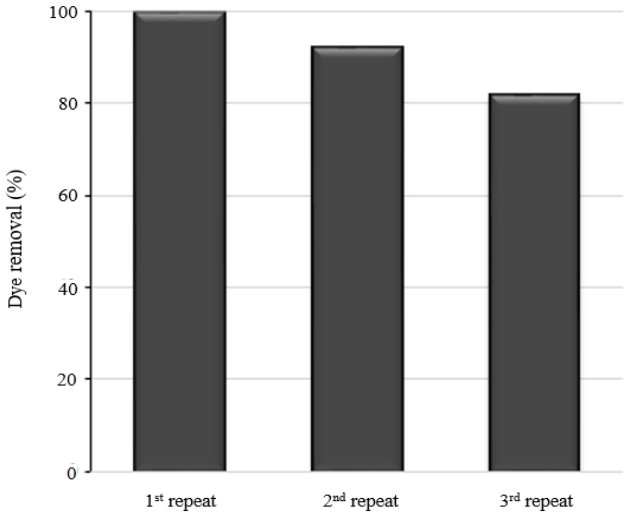

Figure 8. Reusability of TiO_2/20AC in dye removal under UV-light with optimal conditions (acid dye concentration 75 $mg{\cdot}L^{-1}$ reaction time 180 min and catalytic loading 5.0 $g{\cdot}L^{-1}$).

The R^2 of this was in the range of 0.7987-0.9848. The pseudo-first-order kinetics can be used to recognize the adsorption and photo-oxidation mechanisms taking place in the reactor. In case of AC TiO_2 P25 and TiO_2, k_{app} of AC is higher than that of TiO_2 P25 and TiO_2. The k_{app} of TiO_2 with various amounts of AC were significant increased with an increase of AC loading, while the half-life times were reduced. This is due to when the rate constant is increased, which lead to reduction of the reaction time. As mentioned in section 3.7, the adsorption and photocatalytic reaction are continueously reacted by the deposited TiO_2/AC, resulting in hight k_{app} with low half life time. This result supported the synergistic effect phenomena of TiO_2 and AC. Similar results have been reported [16,30].

3.9 Reuse

The reuse of photocatalyst is a significant factor for its practical application in wastewater treatment. The stability of photocatalyst was investigated through recycling of the TiO_2/20AC, which possesses optimal condition in this study. Figure 8 shows the dye removal efficiency with the number of recycling. The removal efficiency was slightly decreased with the number of recycling. At the second cycles, 92.05% of the initial dye was removed after the photocatalytic reaction of 180 min and dropped to 81.76% in the third cycle. The small reduction after each recycle indicates that the TiO_2/20AC is a relatively stable photocatalyst for the photocatalytic dye removal and could be developed into a commercial scale. In case of AC and TiO_2, the dye removal by AC reached 75% at 10 min while photocatalytic removal activity of TiO_2 (P25) was 57%, and that of as-prepared TiO_2 was 26%. In the case of AC, it may be used to remove the dye in only one cycle. For bare TiO_2, there were low dye removal efficiency compare to TiO_2/AC composite.

4. Conclusion

In the present study, photocatalyst TiO_2 with various amounts of AC composites (TiO_2/AC) were synthesized through the sol-gel method. $TiCl_4$ was used as a precursor to reduce using acidic solution during preparation process. Various amounts of AC were introduced as an assistant for a photocatalyst. The catalyst's characterization

showed an even distribution of TiO_2 over the AC surface. The specific surface area of TiO_2 with AC was increased with increasing of mass fraction of AC, while the energy band gap was reduced. The photo-reaction was more effective in the presence of AC than those of TiO_2 and AC alone. The efficiency of the TiO_2/10AC was optimal with 88% dye removal capacity compared with 75% of AC, 57% of TiO_2 (Degussa P25) and 26% of as-prepared TiO_2. The kinetic mechanism of acid dye via photocatalysis was a pseudo-first-order obtained using the Langmuir-Hinshelwood model. Furthermore, the test showed that the reuse of TiO_2/20% AC composite is quite significant, with over 90% efficiency in the recycle. The results thus showed the synergistic effect of TiO_2 and AC and the possibility for the commercial application.

Supplementary data

Supplementary data to this article can be found online at https://doi.org/10.14456/jmmm.2020.xx.

Acknowledgement

This study was financially supported by Farm Engineering and Automatic Control Technology Research group (FEAT group), Applied Engineering for Important Crops of the North East Research group (AENE group), and Sustainable Infrastructure Research and Development Center, Khon Khaen University.

Reference

[1] A. Fujishima, T. N. Rao, and D. A. Tryk, "Titanium dioxide photocatalysis," *Journal of Photochemistry and Photobiology C: Photochemistry Reviews*, vol. 1(1), pp. 1-21, 2000/6/29 2000.

[2] E. Bizani, Fytianos, K., Poulios, I., and V. Tsiridis, "Photocatalytic decolorization and degradation of dye solutions and wastewaters in the presence of titanium dioxide," *Journal of Hazardous Materials, Selected Proceedings of the Seventh Biennial Protection and Restoration of the Environment International Conference*, vol. 136(1), pp. 85-94, 2006/8/10 2006.

[3] H. G. Mobtaker, S. J. Ahmadi, S. M. Dehaghi, and T. Yousefi, "Coupling system application in photocatalytic degradation of methylorange by TiO_2, TiO_2/SiO_2 and TiO_2/SiO_2/Ag," *Rare Metals*, vol. 34(12), pp. 851-858, 2015.

[4] A. C. Martins, A. L. Cazetta, O. Pezoti, J.R.B. Souza, T. Zhang, E. J. Pilau, T. Asefa, and V.C. Almeida, "Sol-gel synthesis of new TiO_2/activated carbon photocatalyst and its application for degradation of tetracycline," *Ceramics International*, vol. 43(5), pp. 4411-4418, 2017.

[5] C. Telegang Chekem, V. Goetz, Y. Richardson, G. Plantard, and J. Blin, "Modelling of adsorption/photodegradation phenomena on AC-TiO_2 composite catalysts for water treatment detoxification," *Catalysis Today*, vol. 328, pp. 183-188, 2019.

[6] Y. Li, S. Li, J. Wang, C. Ma, and L. Zhang, "Preparation and solarlight photocatalytic activity of TiO_2 composites: TiO_2/kaolin, TiO_2/diatomite, and TiO_2/zeolite," *Russian Journal of Physical Chemistry A*, vol. 88(13), pp. 2471-2475, 2014.

[7] X. Zhang, Y. Shen, W. Shi, and X. Bao, "Ethanolic cofermentation with glucose and xylose by the recombinant industrial strain *Saccharomyces cerevisiae NAN-127* and the effect of furfural on xylitol production," *Bioresource technology*, vol. 101(18), pp. 7093-7099, 2010.

[8] M. Lorenzo, D. Moldes, S. R. Couto, and M. Sanromán, "Inhibition of laccase activity from trametes versicolor by heavy metals and organic compounds," *Chemosphere*, vol. 60(8), pp. 1124-1128, 2005.

[9] C. Adán, J. Carbajo, A. Bahamonde, and A. Martínez-Arias, "Phenol photodegradation with oxygen and hydrogen peroxide over TiO_2 and Fe-doped TiO_2," *Catalysis Today*, vol. 143(3), pp. 247-252, 2009.

[10] S. X. Liu, X. Y. Chen, and X. Chen, "A TiO_2/AC composite photocatalyst with high activity and easy separation prepared by a hydrothermal method," *Journal of Hazardous Materials*, vol. 143(1), pp. 257-263, 2007.

[11] L. Andronic, A. Enesca, C. Cazan, and M. Visa, "TiO_2–active carbon composites for wastewater photocatalysis," *Journal of Sol-Gel Science and Technology*, journal article vol. 71(3), pp. 396-405, 2014.

[12] A. Nourbakhsh, S. Abbaspour, M. Masood, S. N. Mirsattari, A. Vahedi, and K. J. D. Mackenzie, "Photocatalytic properties of mesoporous TiO_2 nanocomposites modified with carbon nanotubes and copper," *Ceramics International*, vol. 42(10), pp. 11901-11906, 2016.

[13] B. Gao, P. S. Yap, T. M. Lim, and T.-T. Lim, "Adsorption-photocatalytic degradation of Acid Red 88 by supported TiO2: Effect of activated carbon support and aqueous anions," *Chemical Engineering Journal*, vol. 171(3), pp. 1098-1107, 2011.

[14] K. Blus, "Synthesis and properties of acid dyes derived from 1-phenyl-3-methyl-5-pyrazolone," *Dyes and pigments*, vol. 20(1), pp. 53-65, 1992.

[15] S.H. Madani, C. Hu, A. Silvestre-Albero, M.J. Biggs, F. Rodríguez-Reinoso, and P. Pendleton, "Pore size distributions derived from adsorption isotherms, immersion calorimetry, and isosteric heats: A comparative study," *Carbon*, vol. 96, pp. 1106-1113, 2016.

[16] Y. Li, X. Li, J. Li, and J. Yin, "Photocatalytic degradation of methyl orange by TiO_2-coated activated carbon and kinetic study," *Water research*, vol. 40(6), pp. 1119-1126, 2006.

[17] C. Adán, J. Carbajo, A. Bahamonde, and A. Martínez-Arias, "Phenol photodegradation with oxygen and hydrogen peroxide over TiO_2 and Fe-doped TiO_2," *Catalysis Today*, vol. 143, pp. 247-252, 2009.

[18] J. Zhang, P. Zhou, J. Liu, and J. Yu, "New understanding of the difference of photocatalytic activity among anatase, rutile and brookite TiO_2," *Physical Chemistry Chemical Physics*, vol. 16(38), pp. 20382-20386, 2014.

[19] S. Horikoshi, S. Sakamoto, and N. Serpone, "Formation and efficacy of TiO_2/AC composites prepared under microwave irradiation in the photoinduced transformation of the 2-propanol VOC pollutant in air," *Applied Catalysis B: Environmental*, vol. 140-141, pp. 646-651, 2013.

[20] P. Scherrer and N.G.W. Gottingen, "Math-Pys. Kl.," no. 2, pp. 96-100, 1918.

[21] A. W. Burton, K. Ong, T. Rea, and I. Y. Chan, "On the estimation of average crystallite size of zeolites from the Scherrer equation: A critical evaluation of its application to zeolites with one-dimensional pore systems, *Microporous and Mesoporous Materials*, vol. 117(1-2), pp. 75-90, 2009.

[22] Z. Abbas, J. Perez-Holmberg, A-K Hellström, M. Hagström, J. Bergenholtz, M. Hassellöv, and E. Ahlberg, "Synthesis, characterization and particle size distribution of TiO_2 colloidal nanoparticles," *Colloids and Surfaces A: Physicochemical and Engineering Aspects*, vol. 384(1-3), pp. 254-261, 2011.

[23] F. Rouquerol, J. Rouquerol, and K. Sing, "CHAPTER 1- Introduction," in *Adsorption by Powders and Porous Solids*, F. Rouquerol, J. Rouquerol, and K. Sing, Eds. London: Academic Press, 1999, pp. 1-26.

[24] F.J. Sotomayor, K.A. Cychosz, and M. Thommes, "Characterization of micro/mesoporous materials by physisorption: concepts and case studies," *Accounts Material & Surface. Research*, vol. 3(2), pp. 36-37, 2018.

[25] F. X. Perrin, V. Nguyen, and J. L. Vernet, "FT-IR Spectroscopy of acid-modified titanium alkoxides: investigations on the nature of carboxylate coordination and degree of complexation," *Journal of Sol-Gel Science and Technology*, vol. 28(2), pp. 205-215, 2003.

[26] M. Gar Alalm, A. Tawfik, and S. Ookawara, "Solar photocatalytic degradation of phenol by TiO_2/AC prepared by temperature impregnation method," *Desalination and Water Treatment*, vol. 57(2), pp. 835-844, 2016.

[27] H. Atout, A. Bouguettoucha, D. Chebli, J.M. Gatica, H.Vidal, M.P. Yeste, and A. Amrane," Integration of adsorption and photocatalytic degradation of methylene blue using TiO_2 Supported on granular activated carbon," *Carbon*, vol. 16, pp. 123, 2016.

[28] X.G. Zhao, and L.Q. Huang, "Iridium, carbon and nitrogen multiple-doped TiO_2 nanoparticles with enhanced photocatalytic activity," *Ceramics International*, vol. 43(5), pp. 3975-3980, 2017.

[29] X. Wang, Z. Hu, Y. Chen, G. Zhao, Y. Liu, and Z. Wen, "A novel approach towards high-performance composite photocatalyst of TiO_2 deposited on activated carbon," *Applied Surface Science*, vol. 255(7), pp. 3953-3958, 2009.

[30] M. Vishnuganth, N. Remya, M. Kumar, and N. Selvaraju, "Photocatalytic degradation of carbofuran by TiO_2-coated activated carbon: Model for kinetic, electrical energy per order and economic analysis," *Journal of environmental management*, vol. 181, pp. 201-207, 2016.